PRECISION MASS MEASUREMENTS UTILIZING BETA ENDPOINTS

D.M. Moltz and K.S. Toth

Oak Ridge National Laboratory*), Oak Ridge, Tennessee 37830 USA

F.T. Avignone, III, H. Noma and B.G. Ritchie

University of South Carolina**), Columbia, South Carolina 29208 USA

B.D. Kern

University of Kentucky, Lexington, Kentucky 40506 USA

Abstract

A technique for precise determination of beta endpoints with an intrinsic germanium detector has been developed. The energy calibration was derived from γ-ray photopeak measurements. This analysis procedure has been checked with a ^{27}Si source produced in a (p,n) reaction on an ^{27}Al target and subsequently applied to mass separated samples of ^{76}Rb, ^{77}Rb and ^{78}Rb. Results indicate errors < 50 keV are obtainable.

1. Introduction

Many nuclear and particle physics experiments may be characterized by an attempt to measure the total energy and the energy distribution for a particle or composite group of particles. The total energy of a bound nuclear system is dominated by the mass of the agglomerated particles. Since the masses of the free neutron and proton are known with great precision, the most interesting potential energy part of a nuclear system is the binding energy. Many methods to determine the binding energy of an unknown nuclide have been devised including both direct and indirect measurements. The former tend to give smaller error bars (1-50 keV), while the latter techniques typically yield larger error bars (>50 keV). Because of small cross sections and a lack of suitable target nuclei for direct measurements, indirect methods are dictated. Where observation of radionuclide decay is required, mass separation[1] is often necessary to eliminate as much "background" from competing reaction products as possible. Discrete energy charged particle spectroscopy has long been used to determine both ground state and excited state masses, but this class of nuclei is limited to light neutron-deficient A series, to a small region above Z=50 and to all the well-established alpha-particle emitters above neodymium. Although some mass determinations have been made by utilizing unique systematics, the vast majority of nuclides far from stability require direct beta endpoint measurements which are fraught with inconsistencies due to non-discrete particle energies and to differing detector response functions.

Beta particle detection with plastic scintillators has long been a standard procedure[2,3] with determined mass differences generally having errors > 100 keV. Thus, conversion to intrinsic germanium spectrometers has become an important step in attempts to attain endpoint measurements with errors < 20 keV. The energy calibration is generally much simpler (γ-ray photopeaks may be used), but the response function has been difficult to delineate. This latter problem has been solved in a number of ways, including shape function calculations on known β emitters[4] and empirical electron response function calculations[5] determined from a monoenergetic electron beam. A β spectrometer utilizing a superconducting solenoid to channel the β particles has been constructed[6] and analysis of the detector distorted data has been accomplished through an iterative technique[7]. This technique has been used to measure decay characteristics of ^{78}Rb [8].

Since extra bombardment time for calibrations is not always available, an analysis of the raw electron or positron spectrum distorted by a germanium crystal has been attempted using the γ-ray energy calibration. The basic Monte Carlo approach[9,10] has been successfully used in predicting gamma and negatron spectra as distorted by an intrinsic germanium detector. Further work has been necessary, however, to extend these calculations to positron spectra. Since this work is in the process of being published[11], only a brief synopsis will be given here, in addition to results from the test case ^{27}Si (GS) → ^{27}Al (GS).

The general area between the $f_{7/2}$ and $g_{9/2}$ shells has been only loosely explored. The mass systematics should prove very interesting because of the large number of differing shell model states and because the proton dripline and Z = N line should intersect in this region. In order to utilize the best characteristics of the UNISOR[12] on-line mass separator facility, the direct mass measurements of Ref. 13 and the relative stability of the krypton isotopes to minimize daughter contamination, measurements on the light rubidium isotopes were commenced. Results for ^{76}Rb, ^{77}Rb and ^{78}Rb will be presented.

2. Technique

Although the techniques already mentioned[4,7] have their advantages and seem to work well in interpreting β spectra measured with an intrinsic germanium detector, it was deemed advantageous to develop a technique whereby the energy calibration resultant from γ-ray photopeaks could be utilized. This process would eliminate the necessity for wasting bombardment time on calibrations and simplify the corrections to a standard Fermi-Kurie type calculation.

An attempt to completely calculate the response function of positrons in germanium has been started, but for present purposes a simplified version[11]) has been developed to give positron endpoints. This Monte Carlo calculation simulates the effect of annihilation radiation on the shape of the observed Kurie plot. The code calculates the energy deposited in the detector from both the stopped positron and associated γ rays (511-keV annihilation pairs) and then proceeds to redistribute the peak intensity with a Gaussian smearing routine. All positrons were assumed to stop at the center of the detector. We have found that this assumption does not generally affect the calculated endpoint while it significantly reduces the computer time. The hypothetical detector used in these calculations had dimensions 1.6 cm by 0.7 cm, identical to that used in the measurements described herein. The code was run for theoretical endpoint energies ranging from 2.5 to 9.0 MeV. The calculated energy shift due to annihilation interference (ΔE_0) was found to vary smoothly over this energy range and could easily be fit by the quadratic polynomial[11]):

$$\Delta E_0 = 0.1572 + 0.0115\ E_0 - 0.0007\ E_0^2\ , \qquad (1)$$

where E_0 is the correct endpoint energy. Thus a 4.0-MeV endpoint would be measured as 4.192 MeV. Figure 1 shows a theoretical Kurie plot, an observed Kurie plot and the Monte Carlo simulation for the high energy portion of a known positron emitter (^{82}Rb--see Ref. 11 for details). The slight disagreement on the high energy tail is unimportant for the purpose considered here, since least-squares fits are begun at the point where the Kurie function first becomes linear.

Avoiding the inclusion of data in the nonlinear region of the Kurie was an important consideration in our data analysis. Since this departure from linearity occurs 200 - 300 keV below the endpoint for a detector of these dimensions[11]), a second β-ray branch within this range could create a problem. Unless the statistics of a particular spectrum are very large, this break is not easy to detect. The analysis code thus searches for a consistent endpoint while removing data points in small increments from the high energy side. Removing a small number of data points from the low energy side often changes the endpoint and is probably due either to a second component or to not having properly found the original high energy break. To reduce the statistical error in a particular endpoint measurement, it is necessary to include as much data as possible in the fit. But a second component within the 200-keV break point is non-trivial to treat. A reasonable criterion for data inclusion near the break point has been χ^2 minimization; in principle, data can be added as long as the endpoint remains consistent and χ^2 is reduced. These procedures have been applied where possible to all of the spectra which will be presented.

3. Experimental

The choice of light rubidium isotopes was predicated upon the ease of extracting rubidium from the UNISOR integrated target ion source and the direct mass measurements[13]) which could be used as a basis, or in the case where the krypton daughters are well characterized, provide a check for those same direct mass measurements. It was thus decided to use ^{78}Rb as a check for our technique and commence actual measurements with ^{76}Rb and ^{77}Rb,

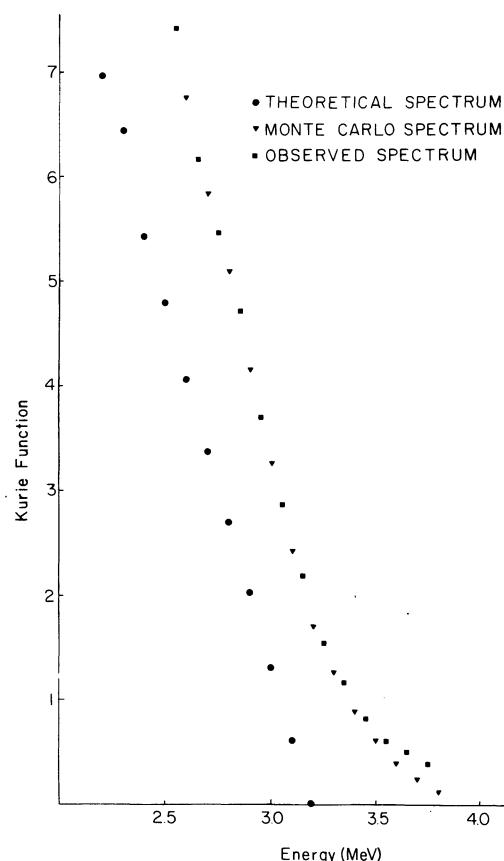Fig. 1 Theoretical, measured and Monte Carlo simulated Kurie plot of high energy positrons arising from the decay of ^{82}Rb.

produced in ^{60,62}Ni(^{20}Ne,pxn) reactions with ^{20}Ne ions accelerated in the Oak Ridge isochronous cyclotron. These reactions are not necessarily the best choice available, but the proximity of the target to the ion source made the choice of a nickel target imperative. Unfortunately, ^{78}Rb has proven to be anything but simple and has not served as the test originally envisioned. Some of the possible reasons will be mentioned later, but a fundamental necessity for such measurements is that the level structure of the daughter be strictly understood. The decay schemes relevant to this work as shown in Fig. 2 are reported in Ref. 14.

A stringent test of both the fitting routines and the Monte Carlo calculations was performed by measuring the ^{27}Si endpoint. Silicon-27 was produced in the ^{27}Al(p,n) reaction with ~ 11.4 MeV protons accelerated in the Oak Ridge EN tandem and then transported to a β-γ coincidence station by a helium-jet system for analysis. A continuous counting-collection cycle was utilized to measure both singles and 511-keV coincidence spectra of the ground state-to-ground state decay. The singles spectrum gave an endpoint of 3983 ± 11 keV and the coincidence spectrum yielded an endpoint of 3980 ± 30 where the errors are strictly statistical. Application of Eq. 1 results in a positron distortion correction of 191 keV which when subtracted
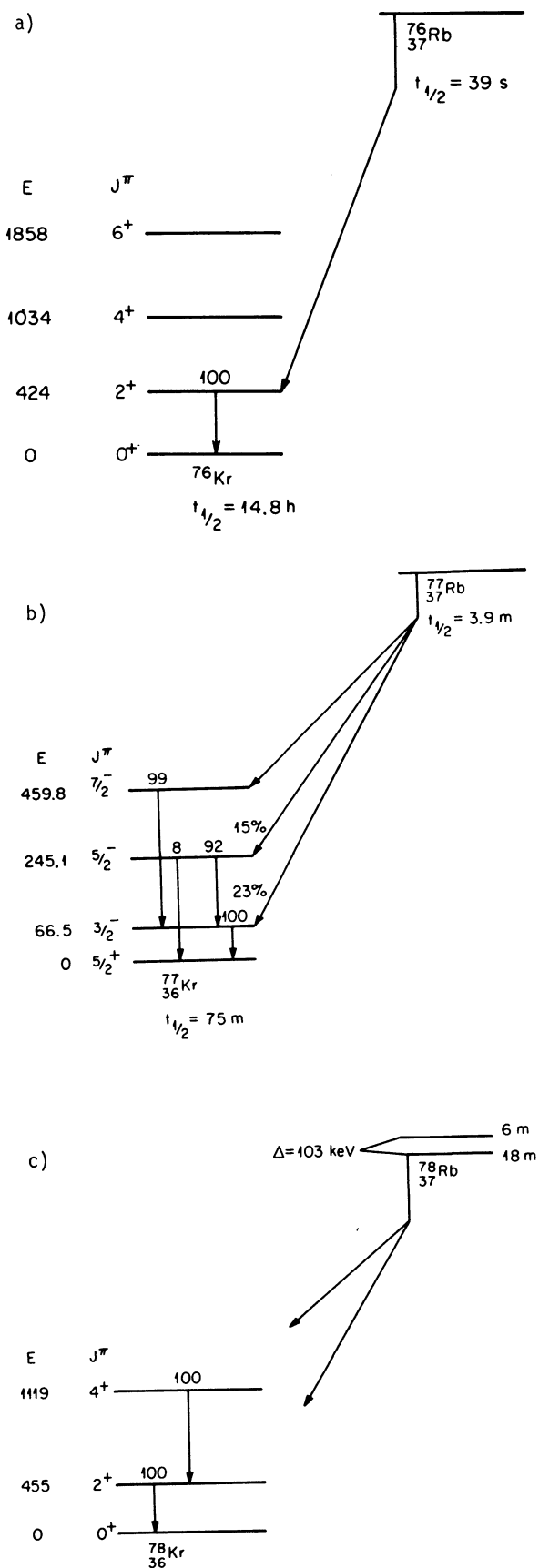
a)

$^{76}_{37}$Rb

$t_{1/2} = 39$ s

E   J$^{\pi}$

1858 6$^+$ ——————

1034 4$^+$ ——————

424   2$^+$ ——100——

0   0$^+$ ——————

^{76}Kr

$t_{1/2} = 14.8$ h

b)

$^{77}_{37}$Rb

$t_{1/2} = 3.9$ m

E   J$^{\pi}$

459.8 7/2$^-$ 99

245.1 5/2$^-$ 8 92   15%

66.5   3/2$^-$ 100   23%

0   5/2$^+$

$^{77}_{36}$Kr

$t_{1/2} = 75$ m

c)

$\Delta = 103$ keV   6 m

$^{78}_{37}$Rb   18 m

E   J$^{\pi}$

1119 4$^+$ ——100——

455   2$^+$ ——100——

0   0$^+$ ——————

$^{78}_{36}$Kr

Fig. 2 Partial decay schemes for a) ^{76}Rb, b) ^{77}Rb
and c) ^{78}Rb, as given in Ref. 14.

yields 3792 and 3789 keV for the final endpoints
for ^{27}Si, in excellent agreement with the accepted
value of 3787.0 ± 1.3 keV [15]). Final errors were
calculated by adding the conservative estimate of
~ 10 keV in the correction factor in quadrature to
the energy calibration error and the statistical
error to give final endpoints of 3792 ± 16 keV and
3789 ± 32 keV for the singles and coincidence
spectra, respectively. The slightly better agree-
ment between our results and previous work[15]) using
the coincidence measurement is expected and such
measurements should be utilized whenever possible.

Although the heavier neutron deficient nuclei
are usually studied first, the order of discussion
will be reversed for the sake of clarity. The
decay of ^{76}Rb had been previously studied[16,17]) and
the simple decay scheme shown in Fig. 2 is con-
sistent with our observation. A Kurie plot of the
singles spectra for ^{76}Rb is shown in Fig. 3. Since
the ion source produces no ^{76}Kr or ^{76}Sr and since
^{76}Kr emits no β^+ particles, the measured spectrum
was completely attributable to ^{76}Rb. Essentially
no events were recorded above 5 MeV (8 MeV was the
collection limit). The 2$^+$ → 0$^+$ and 4$^+$ → 2$^+$ transi-
tions in ^{76}Kr are 424 and 612 keV, respectively.
No evidence for the latter transition was observed,
whereas most of the beta strength seemed to be
channeled through the 2$^+$, 424-keV level. Analysis
of these data provides an excellent illustrative
example of the ideal analysis procedure. Using a
distortion break at ~ 4250 keV garnered from the
singles spectrum, a series of fits was obtained by
using a progressively larger data base. Fits were
terminated when the endpoint obtained was no longer
consistent. The final endpoint of 4584 ± 40 keV
in Table 1 was chosen on the basis of the minimum
χ^2 utilizing a 1000-keV range of data. Slightly
differing ranges for fits could have been chosen,
but would not have had a significant effect on the
final value. This is clearly a best-case example
and, as will be shown, other fits obtained are not
quite as simple.

Table 1

^{76}Rb β^+ Decay — 424-keV Gamma Gate Fits

Range from Distortion Break in Kurie Plot (keV)	Endpoint	Relative Chi-square
600	4579	1.08
800	4583	1.03
1000	4584	1.00
1200	4584	1.13
1500	4500	1.12

The spectrum of positrons in coincidence with
annihilation radiation yield an endpoint of
4585 ± 42 keV. After correcting for annihilation
radiation distortion, adding in the γ-ray energy
and taking appropriate averages, a final Q_{EC} of
5835 ± 42 keV was obtained. The singles spectrum
yielded a Q_{EC} of 5833 ± 16 keV. Results from all
three analyses are summarized in Table 2. It
should also be noted that a lack of a ground state
positron branch, in addition to the unobserved
4$^+$ → 2$^+$ transition suggest that the ground state
spin and parity of ^{76}Rb is 2$^+$, in accordance with
Ref. 17.

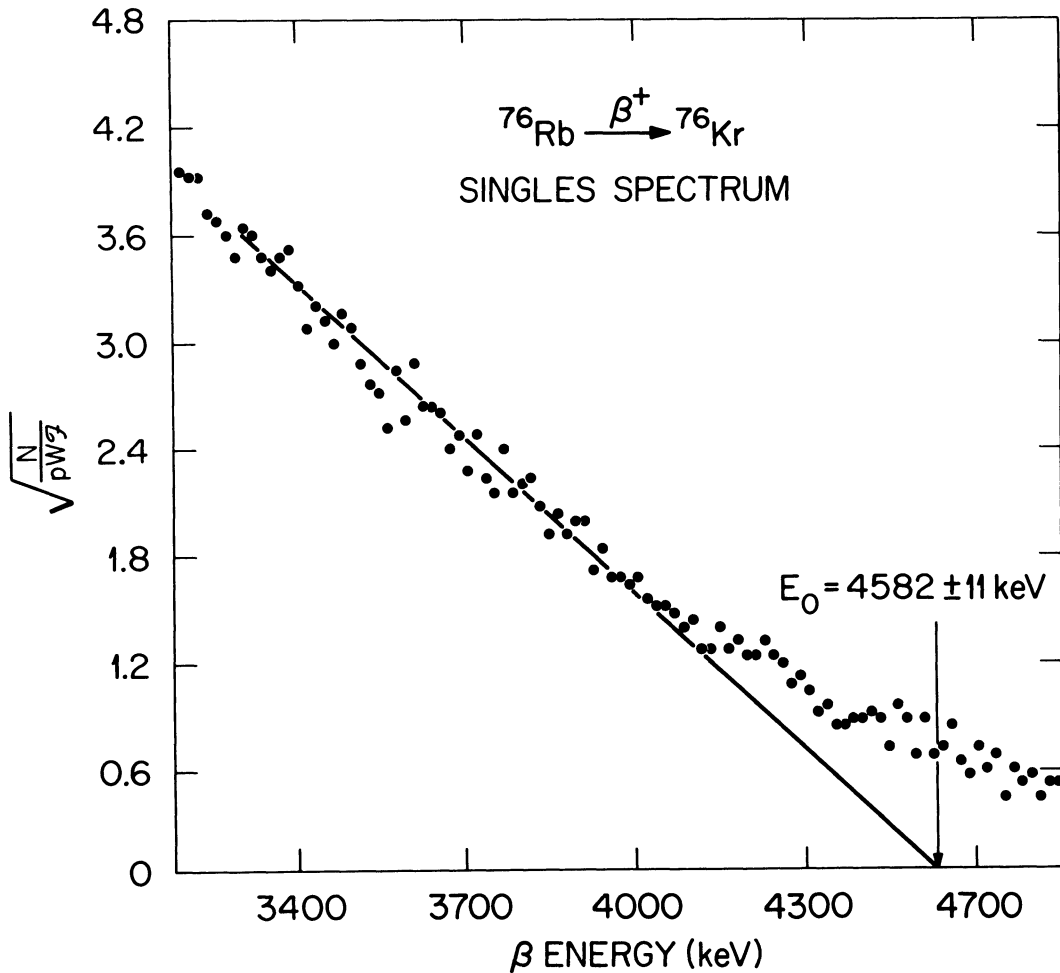Fig. 3 High-energy singles positron spectrum arising from the decay of [76]Rb.

Table 2

[76]Rb Endpoint Results

	Gamma Gate (keV)		Singles
	424	511	
Measured E_0 (keV)	4584±40	4585±42	4582±11
Annihilation Radiation Correction (keV)	-195	-195	-195
Gamma Energy (keV)	424	424	424
Q_{β^+} (keV)	4813	4814	4811
Weighted Mean (keV)	4813±30		
Q_{EC} (keV)	5835±42		5833±16

Because the high cross section $^{60}Ni(^{20}Ne,2pxn)$ reactions are hindered when x = 0 or 1, this permits a greater yield for the $^{60}Ni(^{20}Ne,p2n)$ reaction as a percentage of the total reaction cross section. This larger yield is useful because the fragmented decay of ^{77}Rb (see Fig. 2) requires greater statistics. Furthermore, the five γ rays (66, 179, 245, 394 and 511 keV) should provide five independent measurements of the same value. Choice of data fitting region was much more difficult because of the level spacing, particularly for the 66-keV transition. Since the positron end-point for ^{77}Kr is ~ 2 MeV, positrons from the ^{77}Kr daughter should not interfere. Thus, the only convergence criteria used were that the 66- and 511-keV gated spectra should yield the same endpoint and that the 179- and 245-keV gated spectra should also give the same endpoint. An attempt was made to obtain a consistent endpoint using only a 150- to 250-keV range below the distortion break in the Kurie plot for the 66- and 511-keV gated spectra and to minimize both χ^2 and the statistical error bar within the context of a very limited amount of data. Thus, a consistent endpoint utilizing the same analysis procedures as for ^{76}Rb was not possible. Instead, an endpoint sometimes had to be based on an average of all similar endpoints with consistent χ^2 values and statistical error bars because no particular subset of data could clearly be called best. For example, with the 245-keV gated data, reasonable fits for slightly differing energy ranges gave several endpoints with similar χ^2 values. The final value was taken to be a simple average with the largest statistical error, 4023 ± 28 keV. This value is consistent with the 179-keV result of 4026 ± 18 keV. This averaging procedure was used only in the cases of the singles spectrum and the 66-, 245- and 394-keV gated spectra.

Figure 4 gives the Kurie plot for the high energy 179-keV gated data. This plot shows the annihilation radiation distortion break, but only the singles spectrum makes it clear enough to choose a fitting region (as can be seen in the singles spectrum for ^{76}Rb in Fig. 3). Furthermore, most gated spectra do not have sufficient statistics to delineate this point. Therefore, careful analysis was required to discover where the fit should begin. This problem was particularly acute for the 66-keV gated data, where the final value of 4212 ± 28 could easily be calculated as 5-10 keV higher, but the 511-keV gated data could in no reasonable manner give such values and convergence was a necessary criterion. Table 3 summarizes our
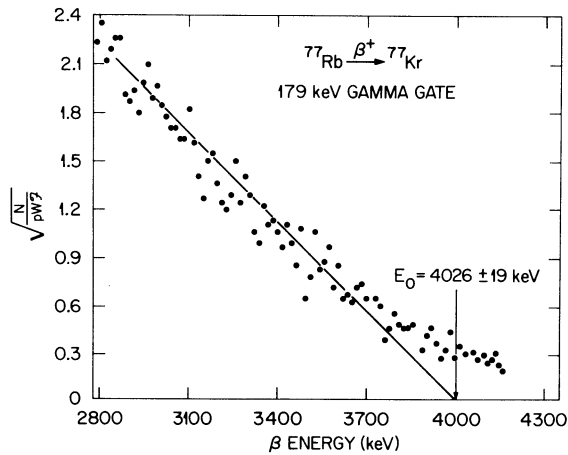

Fig. 4 Kurie plot of the 179-keV gated data from the decay of ^{77}Rb.

distortion break. Obviously, singles spectra can only be used for special cases where no radio-activities (including the daughter) have endpoints above or in the same range as the nuclide of interest. It is also imperative to know the relevant decay scheme precisely for calculating proper endpoints; however, an endpoint can also be used to locate a particular energy level in the daughter nucleus.

The plan to utilize ^{78}Rb as a preliminary check was quickly shattered once the data were obtained. Figure 5 compares the singles and 455-keV gated positron spectra. It should be immediately evident that the endpoints of these two spectra differ by more than the 455 keV suggested by the decay scheme in Fig. 2. The 511-keV gated data also shows the very high energy trend, but because of the very small number of events, valid endpoints are not attainable. The final fitting range for the 455-keV gated data yields a corrected endpoint of 3150 ± 110 keV. This value was corroborated by fitting the equivalent range of 511-kev gated data, yielding 3160 ± 85 keV. Previously, the endpoint[16] for ^{78}Rb has been obtained by gating on the 664-keV transition. Our final endpoint for this data of 2480 ± 70 keV is consistent with the decay scheme given in Fig. 2, but is not consistent with that given in Ref. 16 of 3410 ± 370 keV.

Although the singles spectrum high energy statistics are extremely poor (<10% of decay strength), a crude endpoint of 6060^{+300}_{-170} shows that perhaps previous decay scheme work[18-20] was incorrect. Recent work by Rehfield and Moore[8] give an endpoint of 6221 ± 20 as being due to a 0^+ (GS) → 0^+ (GS) isospin forbidden beta transition

Table 3

^{77}Rb Endpoint Results

	Gamma Gate (keV)				
	66	511	179	245	394
Measured E_0 (keV)	4212±28	4208±46	4026±18	4023±28	3812±35
Annihilation Radiation Correction (keV)	-193.5	-193.5	-192.0	-192.0	-190.6
Gamma Energy (keV)	66.5	66.5	245	245	450.8
$Q_{\beta}+$ (keV)	4085±30	4081±48	4079±21	4076±30	4081±37
Weight = $\sqrt{N}$	35	34	85	60	37
Weighted Mean (keV)			4080±13		
Q_{EC} (keV)			5102±25		
Singles Q_{EC} (keV)			5103±15		

observations, including a final value for Q_{EC} of ^{77}Rb of 5102 ± 25 keV. The excellent agreement of the value derived from the singles spectrum only serves to indicate that in some cases good endpoints can be derived from such spectra. It should not be construed as a better measurement. The quoted error bars are based solely on statistics of the ~ 150-keV fitting range from the positron

with a log ft value of 7.95. Since their measurement was begun after waiting 45 min to eliminate any 6 min ^{78m}Rb decays and because the sample was produced in the ^{78}Kr(p,n) reaction at 15 MeV, these beta particles must be from ^{78g}Rb. For reasons already elucidated, our sample was also pure ^{78}Rb, forcing the beta decays involving the 455- and 664-keV transitions to occur elsewhere in ^{78}Kr,
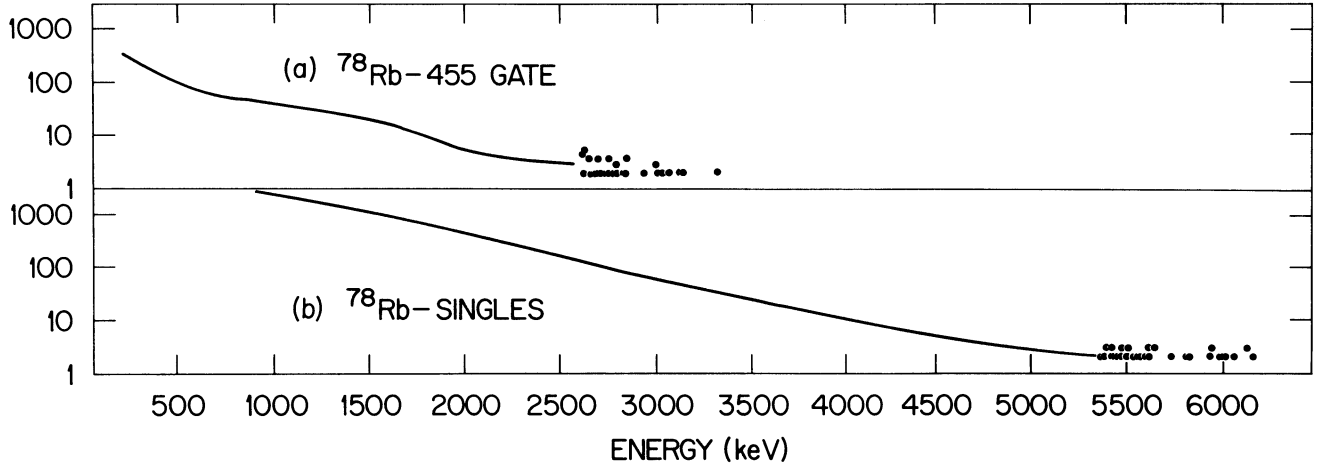
Fig. 5 Raw beta spectra observed in the decay of ^{78}Rb: a) 455-keV gated data, b) singles data.

transitions to occur elsewhere in ^{78}Kr, or necessitating a search for some very high energy γ transitions. Work on a more detailed decay scheme for ^{78}Rb is under way[21]) and it is hoped this will clarify these matters. Our present results thus tend to support the conclusions of Ref. 8.

4. Results and Conclusions

Although our values for Q_{EC} for ^{77}Rb and ^{76}Rb should be considered preliminary, the base numbers should change little. The error bars should also be considered preliminary, with the statistical error dominating. Table 4 summarizes our results and also compares them with the direct mass measurements of Ref. 13. The decay energy for ^{77}Rb agrees well with one scintillator measurement[16])

(5180 ± 390 keV), but not with another[23]) (4882 ± 150 keV). Furthermore, within quoted error bars, our value agrees with the direct mass measurements[13]), but the ~ 100 keV difference is of opposite sign from that in ^{78}Rb. These differences are noted because the direct mass measurements have been called into question[26,27]).

The measured decay energy for ^{76}Rb is lower than most all predictions by ~ 2.5 MeV. Since the observed ^{76}Rb spectrum (unlike ^{78}Rb) indicated no significant high energy events, any large error in the reported spectroscopy would necessitate either a ground state-ground state transition with a branching ratio less than 1% or a different location for the 424-keV transition in ^{76}Kr. The error in the direct mass measurements does not account for this discrepancy. Unfortunately, the mass for

Table 4

Final Q_{EC} and Mass Excess Values

Nuclide	^{78}Rb	^{77}Rb	^{76}Rb
Q_{EC} (keV)	7242±20[a])	5102±25[b])	5835±42[b])
Direct Mass Measurement[c]) Mass Excess (keV)	-67076±64	-65037±105	-60668±151
A	78	77	76
Mass Excess of Kr Isotopes (keV)[d])	-74150±8	-70236±30	-69100±200[e])
Derived Rb Mass Excess ($M_{(Kr)}$ + $Q_{EC(Rb)}$) (keV)	-66908±22	-65134±39	-63265±205
Difference from Direct Measurements (keV)	168	-97	-2597

a) Ref. 8.
b) This work.
c) Ref. 13.
d) Ref. 15.
e) Based on Ref. 22.

^{76}Kr has been measured only indirectly[22]) by observing the endpoint of delayed protons from the decay of ^{77}Sr. Clarification of all these bits of information will require two more important links--the mass of ^{76}Kr and better spectroscopic information in the decay of ^{76}Rb. The latter problem has been given a cursory inspection[28]) with no real surprises. The first problem is currently under study here at Oak Ridge.

Another possibility which might explain the small Q_{EC} for ^{76}Rb is the correctness of the response of our detector to higher positron energies. Data have been obtained on the decay of ^{58}Cu [15]) $(Q_{\beta+})$ = 7540.6 ± 2.4 keV and, although analysis is incomplete, the raw beta spectrum suggests the decay energy is within 100 keV of this number. Since a natural nickel target was used in the (p,n) reaction bombardments $(E_p$ = 11.4 MeV), ^{60}Cu data were also obtained simultaneously. These spectra should provide a clue as to the validity of subtracting one component to obtain a second endpoint. If this technique is successful with ^{58}Cu and ^{60}Cu, then it will be applied to the ^{77}Kr contribution present as a low energy background in the ^{77}Rb spectra. An accurate decay energy for ^{77}Kr will provide a complete chain to ^{77}Br whose mass is known[29]) to 3.8 keV from (p,n) threshold reactions.

Our measurements for ^{77}Rb and ^{76}Rb appear consistent with predictions[11]) and thus questions arise about how these Q_{EC} values fit into the general nuclear mass surface systematics. It is clear, however, that much work remains.

References

1) P.G. Hansen, Ann. Rev. Nucl. Part. Sci. 29 (1979) 69.

2) H. Otto, P. Peuser, G. Nyman and E. Roeckl, Nucl. Instr. Meth. 16 (1979) 507.

3) E. Beck, Nucl. Instr. Meth. 76 (1969) 77.

4) R.C. Pardo, C.N. Davids, M.J. Murphy, E.B. Norman and L.A. Parks, Phys. Rev. C15 (1977) 1811.

5) R. Decker, K.D. Wünsch, H. Wollnik, E. Koglin, G. Siegert and G. Jung, Z. Phys. A294 (1980) 35.

6) R.B. Moore, S.I. Hayakawa and D.M. Rehfield, Nucl. Instr. Meth. 133 (1976) 457.

7) D.M. Rehfield, Nucl. Instr. Meth. 157 (1978) 351.

8) D.M. Rehfield and R.B. Moore, to be published in Phys. Rev. C.

9) T.A. Girard and F.T. Avignone, III, Nucl. Instr. Meth. 154 (1978) 199.

10) F.T. Avignone, III, L.P. Hopkins and Z.D. Greenwood, Nucl. Sci. Eng. 72 (1979) 216.

11) F.T. Avignone, III, H. Noma, D.M. Moltz and K.S. Toth, to be published in Nucl. Instr. Meth.

12) UNISOR is a consortium of 13 institutions and is supported partially by them and by the U.S. Department of Energy under Contract No. DE-AC05-760R00033 with Oak Ridge Associated Universities.

13) M. Epherre, G. Audi, C. Thibault, R. Klapisch, G. Huber, T. Touchard and H. Wollnik, Phys. Rev. C19 (1979) 1504.

14) Table of Isotopes, 7th Edition, C.M. Lederer and V.S. Shirley, eds. (John Wiley & Sons, New York, 1978).

15) A.H. Wapstra and K. Bos, At. Data Nucl. Data Tables 19 (1977) 175.

16) L. Westgaard, K. Aleklett, G. Nyman and E. Roeckl, Z. Physik A275 (1975) 127.

17) D.D. Bogdanov, I. Voboril, A.V. Dem'yanov, V.A. Karnaukhov and L.A. Petrov, Iz. Akad. Nauk SSSR. Ser. Fiz. 39 (1975) 2029.

18) E. Nolte and Y. Shida, Z. Physik 256 (1972) 243.

19) J. Chaumont, E. Roeckl, Y. Nir-El, C. Thibault-Phillipe, R. Klapisch and R. Bernas, Phys. Lett. 29B (1969) 652.

20) J.A. Velandia, W.I. Holmes and G.G.J. Boswell, J. Inorg. Nucl. Chem. 34 (1972) 401.

21) J. Crawford, private communication.

22) J.A. Hardy, J.A. MacDonald, H. Schmeing, T. Faestermann, H.R. Andrews, J.S. Geiger, R.L. Graham and K.P. Jackson, Phys. Lett. 63B (1976) 27.

23) Ya. Liptak and W. Habernicht, Iz. Akad. Nauk SSSR. Ser. Fiz. 39 (1975) 501.

24) S. Thulin, Ark. Fys. (Sweden) 9 (1955) 137.

25) K.A. Baskova, S.S. Vasil'ev, M.A. Mokhsen, T.V. Chugai and L. Ya. Shavtvalov, Iz. Akad. Nauk SSSR. Ser. Fiz. 37 (1973) 73.

26) A.H. Wapstra and K. Bos, in Atomic Masses and Fundamental Constants 6, Jerry A. Nolen,Jr. and Walter Benenson, eds. (Plenum, New York, 1980) p. 547.

27) A.H. Wapstra, in Future Directions in Studies of Nuclei Far From Stability, J.H. Hamilton et al., eds. (North Holland, Amsterdam, 1980) p. 209.

28) J. Lin, private communication.

29) C.H. Johnson, A. Galonsky and J.P. Ulrich, Phys. Rev. 109 (1958) 1243.